Journal of Materials Chemistry A

Accepted Manuscript

ROYAL SOCIETY OF CHEMISTRY

www.rsc.org/materialsA

Journal of Material Chemistry A

ARTICLE

Al-coordination polymers-derived nanoporous nitrogen-doped carbon microfibers as metal-free catalysts for oxygen electroreduction and acetalization reaction

Received 00th January 20xx,
Accepted 00th January 20xx

DOI: 10.1039/x0xx00000x

www.rsc.org/

Zhen Han[a,b], Youyi Yu[a],Yongbo Zhang[a], Bing Dong[a], Aiguo Kong*[a] and Yongkui Shan*[a]

Nanoporous nitrogen-doped carbon microfibers were facilely synthesized by the pyrolysis of coordination polymer microfibers of aluminium-diethylenetriamine pentaacetatic acid (Al-DTPA). Al-DTPA microfibers could be easily produced at a scale of over 0.25 kilograms by a homogeneous precipitation reaction of DTPA and aluminium nitrates in aqueous solution. After undergoing thermal conversion of Al-DTPA at the optimized temperatures and acid-leaching, the well-defined nitrogen-doped carbon microfibers were obtained at a scale of over 10 g in laboratory. The interconnected nanoporous textures and plentiful nitrogen-doped functional sites endow such microfibers not only efficient catalytic activity for oxygen reduction reaction (ORR) in 0.1 M KOH electrolyte, but also superior durability and methanol-tolerance during ORR. Moreover, Al-DTPA microfibers could be also transferred into carbon-based nanoporous solid acids by the sulfuric acid-sovothermal treatment. Plentiful of -SO_3H functional groups were grafted on the surfaces of nanoporous nitrogen-dopped carbon microfibers (protonic acid amount,1.8 mmol/g). It served as a highly efficient and recyclable solid acid catalyst for the acetalization of benzaldehyde and ethylene glycol in a yield of about 99.0 at%. The thermal conversion of Al-coordination polymers might be a new practically feasible technique for the preparation of functional nanoporous nitrogen-doped carbon microfibers.

1 Introduction

Because of the excellent physical and chemical properties including exceptional stiffness and strength, extraordinary resistance to corrosion, remarkable thermal and electrical properties, and low density, carbon materials were demonstrated as the promising adsorbents, catalyst supports, electrodes, sensors, and hydrogen storage materials.[1-6] Recently, functionalized carbon materials have been especially investigated as metal-free catalysts in the heterogeneous acid catalysis and oxygen reduction reaction (ORR) occurring at the cathode of Li-O_2 or H_2-O_2 cells.[7-12] Doping nitrogen atoms into the carbon matrixes can break the electric uniformity of carbon framework and creat the ORR active sites with higher electron density.[13-20] Profiting from the additional high electron density of nitrogen-doped carbons, more protonic acid sties (-SO_3H) can be formed in the sulfonation.[21-23] As a result, the nitrogen-doped carbon materials have highly efficient catalysis activity for ORR and can be used as effective supports for protonic acid sties.[24,25]

The morphology, surface chemistry, and local pore structure of nitrogen-doped carbon materials generally need to be synergistically tuned for enhancing catalytic performance of electrode materials and solid acids. The hierarchical porosity of nitrogen-doped carbons can usually provide a larger accessible specific surface area and volume of pore, which will facilitate the transportation and penetration of electrolyte and substrates and increase the density of active sites on their surface in the heterogeneous reaction.[7,26-31] Among different morphologies of carbon materials, one-dimensional microfiber is a practically promising morphology in the assembling of membrane electrodes. In particular, due to its easy collection property from the solution by the filtration, it can also act as the easily recycled heterogeneous catalysts.[26,31-36] Nitrogen-doped carbon microfibers (NCFs) with hierarchical porosity may be developed as the practical ORR electrocatalysts or protonic acid supports.

NCFs have been generally synthesized by electrospinning [37-40] and chemical vapour deposition (CVD).[41-43] The CVD method using metal as seeds or catalysts could prepare NCFs with high degree of graphitization, but with low porosity and yield. The metal contaminants in products caused much confusion to understand the origin of ORR activity. Lower yield of carbon products also caused much difficulty in the practical mass production. For the NCFs obtained by the electrospinning techniques, they usually possessed very low degree of graphitization,[37,44-45] which would often lead to insufficient electroconductivity and strength. It may hinder the

[a] School of Chemistry and Molecular Engineering, East China Normal University, 500 Dongchuan Road, Shanghai 200241, P.R. China.
[b] Shanghai Key Laboratory of Molecular Catalysts and Innovative Materials, Fudan University, Shanghai 200433, P.R. China.
[c] † Footnotes relating to the title and/or authors should appear here.
Electronic Supplementary Information (ESI) available: [details of any supplementary information available should be included here]. See DOI: 10.1039/x0xx00000x

transportation of electron in eletrocatalyst and the stability of -SO_3H on the supports. More importantly, it has much difficult in achieving the fine control of surface area, pore size, and surface functionality for the prepared NCFs by both methods.[37-40] The formed pores in microfibers prepared by both methods are often inner pores with small pore sizes (<2 nm), which is adverse to the mass transportation in catalytic reactions. It is of great interest to achieve an optimized balance between microfiber morphology, pore structure, surface area, degree of graphitization, and the content of nitrogen in the carbon material by an available synthesis technique in the practical application.

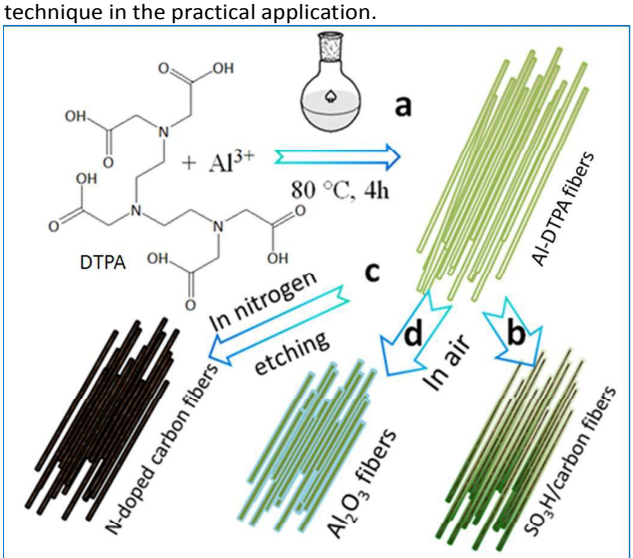

Figure 1. Schematic illustration of the formation process of the nanoporous N-doped carbon microfibers and microfiber solid acids

Hard-templating method may be an ideal synthesis technique to prepare porous carbons with relatively higher degree of graphitization.[7,9,46-48] However, nitrogen-doped carbon microfiber is rarely reported by this synthesis method,[34-36,49] because the synthesis of porous microfiber hard-templates in itself is also very difficult. More recently, the directed thermal conversion of metal-organic frameworks (MOFs) or coordination polymers (CPs) is used as an alternative synthesis route to obtain various carbon materials. Porous carbons with special morphology such as cube and polyhedron etc. could be synthesized by this method,[50-54] and their pore structures may be easily tuned by the as-formed metal or metal oxide nanoparticles. But it is worrying in the high-cost of MOFs and CPs and the resultant carbons.[50-51,55,56] Herein, a simple and scalable aqueous co-precipitation synthesis strategy (Figure 1) could be used to prepare aluminium(Al)-diethylenetriamine pentaacetatic acid (DTPA) coordination polymer(Al-DTPA) microfibers, which are inexpensive, easily-synthesized, and effective precursors for the preparation of NCFs by thermal-conversion. The Al-DTPA-derived NCFs were demonstrated to be efficient metal-free electrocatalysts for ORR in alkaline medium. Moreover, -SO_3H acid groups can be efficiently grafted on NCFs by a sulfonation process. The resultant SO_3H/NCFs were highly effective and recycled carbon-based solid acids for the acetalization reaction of benzaldehyde with ethylene glycol.

2 Experimental

2.1 Synthesis of NCFs

585 g of DTPA and 563 g of $Al(NO_3)_3{\cdot}9H_2O$ were dissolved into 12 L deionized water in a glass reaction vessel of 20 L equipped with a mechanical agitation. The reaction solution was heated at 80 °C for 4 h. The resulting white Al-DTPA microfibers were easily separated by filtration. The collected filtrate can be re-used in the next run of Al-DTPA production. The obtained Al-DTPA microfibers are about 250 g. After that, the dried Al-DTPA microfibers were heated to the desired temperatures in the temperature range of 750-1000 °C with a heating rate of 2 °C min^{-1} and hold for 4h in a quartz tube furnace (Diameter, 8 cm) under nitrogen atmosphere. Finally, the NCFs were obtained by etching off Al_2O_3 or $Al(OH)_3$ materials with an aqueous solution of hydrogen fluoride (HF, 5 wt%) or hydrochloric acid(HCl,10 wt%) or sodium hydroxide (NaOH,10 wt%). The prepared samples are assigned to NCF-n (n is the thermal-treatment temperature)

2.2 Synthesis of sulfonated NCFs

The carbonized Al-DTPA microfibers were sulfonated by a traditional synthesis technique. Typically, the Al-DTPA fibers carbonized at different temperatures (1.0 g) were added into 20 mL of concentrated sulfuric acid, and the resultant mixtures were heated at 180-185 °C for 12 h in a round-bottom flask with a refluxing condenser under a dry N_2 atmosphere. After cooling to room temperature, the mixture was diluted with distilled water. The black precipitate was collected by filtration and rinsed thoroughly with hot distilled water (>80 °C) to remove impurities such as sulfate ions. The resulting black solid catalysts were dried at 80 °C for 10 h in vacuum. The as-prepared sulfonated carbon microfiber catalysts are denoted to SO_3H/NCF-n (n is the heat-treatment temperature in the carbonization procedure).

2.3 Characterization

Powder X-ray diffraction patterns (XRD) were recorded on a D8 Advance X-ray diffractometer (Bruker AXS, Germany) with CuKα radiation. Transmission electron microscope (TEM) images were obtained on a JEOL-2010 transmission electron microscope at an acceleration voltage of 200 kV. N_2 adsorption/desorption measurements were carried out at 77 K on a Micromeritics ASAP 2020M analyzer. Specific surface areas were calculated by the Brunauer-Emmett-Teller (BET) and T-plot method, and the pore size distributions were calculated from the related adsorption isotherms by using the Barrett-Joyner-Halenda (BJH) model. X-ray photoelectron spectroscopy (XPS) measurements were performed on Axis Ultra DLD using C 1s (284.8 eV) as a reference to correct the binding energy. Thermogravimetric analysis (TGA) was carried out using a Perkin Elmer Diamond thermogravimetric analyzer; the samples were analyzed in an air atmosphere and a temperature range from room temperature to 800 ˚C, with a

heating rate of 10°C min^{-1} and an air flow rate of 10 ml min^{-1}. A Hitachi ST-4800 scanning electron microscope (SEM) was used to determine the catalyst morphology. Fourier transform infrared (FT-IR) spectra were recorded on a Nexus-870 Fourier-transform spectrophotometer using KBr pellet technique with a measuring range of 400-4000 cm^{-1}. Component elements were analyzed on elemental analyses on a Perkin-Elmer series II 2400 CHNS Analyzer. The densities of -SO_3H groups were estimated based on the sulfur content obtained by elemental analysis. The SO_3H+COOH content and total amount of acid (SO_3H+COOH+OH) were estimated from the exchange of Na+ in aqueous NaCl and NaOH solutions, respectively.[57] Based on these results, the amount of each functional group can be obtained.

2.4 Electrochemical measurement

The electrocatalytic activities of the as-prepared catalysts for ORR were evaluated by cyclic voltammetry (CV) and rotating disk electrode (RDE) techniques on a CHI-800C electrochemical analyser. A standard three-electrode cell was employed using a glassy carbon RDE (5mm in diameter, Pine) as working electrode, an Ag/AgCl, KCl (3 M) electrode as the reference electrode, and a Pt wire electrode as the counter electrode. The ORR experiments performed in alkaline electrolyte were carried out in 0.1 M KOH solution and the potential range was swept between -1.0 and +0.1 V at a scan rate of 10 mV s^{-1} at the ambient temperature and after first purging with O_2 or Ar gas for 20 min. Commercial 10 wt% Pt/C catalysts obtained from Alpha Acesar were used as a point of comparison. All of the working electrodes were prepared as following: 10 mg of catalysts was dispersed in a solution containing 1.2 mL ethanol and 0.08 mL 5 wt% Nafion-isopropanol solution, followed by ultra-sonicating the mixture for 30 min. The prepared catalyst ink was pipetted onto a glassy carbon electrode surface (0.196 cm^2), polished by alumina suspension (0.05 μm). The final electrode was dried at room temperature. The catalyst loading of active NCFs on the working electrode is 0.2 mg cm^{-2}. For Pt/C, the loading of active material is 0.1 mg (Pt-C) cm^{-2}. All of the potentials (vs Ag/AgCl) have been converted to the potentials vs the reversible hydrogen electrode (RHE) potentials. The Koutecky-Levich (K-L) equations[58], were used to calculate the kinetic parameters of ORR on the tested materials:

$$\frac{1}{J} = \frac{1}{J_L} + \frac{1}{J_K} = \frac{1}{B\omega^{1/2}} + \frac{1}{J_K};$$

$$B = 0.62nFC_0(D_0)^{2/3}\upsilon^{-1/6};\ J_K = nFkC_0$$

, in which J, J_K and J_L are the measured current density, kinetic- and diffusion-limiting current densities, respectively; n, ω and F are the number of electrons transferred during ORR, the angular velocity of the disk, and the Faraday constant (F=96485 C $mol\ L^{-1}$), respectively. C_0 is the bulk solubility of O_2, D_0 is diffusion coefficient of O_2, ν is the kinematic viscosity of the electrolyte, and k is the electron transfer rate constant.

2.4 Acetalization reaction over sulfonated NCFs

In a typical acetalization reaction, ethylene glycol (EG) of 2.79 g (45 mmol) and benzaldehyde (PhCHO) of 1.59 g (15 mmol) were added in cyclohexane of 5.0 g (59.2 mmol), and then as-prepared SO_3H/NCF-600 materials of 30 mg were added into the solution. After that, the reaction mixtures were refluxed for 1 h at about 90 °C in a 50 ml three-necked flask equipped with the Dean-Stark apparatus. At the end of reaction, SO_3H/NCF-600 catalysts were recovered by simply decanting the reaction solution, washing with water and ethanol and drying the used catalysts at 100 °C for 2 h between cycles. The products were analysed by using toluene as the internal standard material on LINGHUA-9890A gas chromatograph (GC) instrument with an OV-1 capillary column of 50 m and an FID detector.

3 Results and discussions

3.1 Synthesis and characterization of Al-DTPA microfibers

The formation of Al-DTPA microfibers is the key step in the preparation of NCFs and microfiber carbon acid catalysts. In the presented synthesis here, Al-DTPA was very facially obtained by reacting $Al(NO_3)_3$ salts with DTPA in an aqueous solution (Figure 2a). It is a homogeneous precipitation reaction occurring at lower temperature (80 °C) for the short reaction time (4 h). The Al-DTPA microfibers can be produced at a scale of several grams to several hundred grams in laboratory. Unlike the hydrothermal synthesis of MOFs and CPs reported in the literature,[51,55] the synthesis of Al-DTPA is very cost-effective and environment-friendly. There are no any additional agents and no special equipment is required in the synthesis. The residual filtrate containing reactants can be reused in the next run of Al-DTPA preparation. The Al $(NO_3)_3$ and DTPA are also cost-effective raw materials.

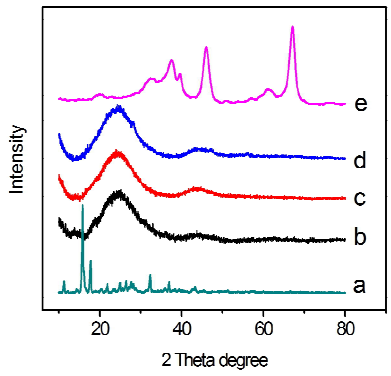

Figure 2 XRD patterns of as-prepared Al-DTPA coordination compounds (a), NCFs obtained at 750 (b), 900 (c) and 1000 °C (d), and Al_2O_3 microfibers obtained by heating Al-DTPA at 800 °C in air (e).

The prepared Al-DTPA microfibers are highly crystalline, and the corresponding strong diffraction peaks in the XRD patterns can be markedly observed (Figure 2 a). Typical microfiber morphology for Al-DTPA was clearly observed by SEM and TEM (Figure 3). The lengths of them are about 50-60 μm with the diameters of ~300-500 nm (Figure 3A and Figure S1). The diameter or length of Al-DTPA can be tuned by changing the

precipitation reaction temperatures and molar ratios of DTPA to $Al(NO_3)_3 \cdot 9\ H_2O$. (Figure S2). The C (39.2 wt%) and N (9.7 wt%) content for Al-DTPA determined by element analysis reveal that the molar ratio of C to N is about 4:1, which suggests that molecule structure of DTPA could be almost maintained in the Al-DTPA products. The FT -IR bands of DTPA at 2937, 1700, 1660, 1396 and 1242 cm^{-1}, which are relevant to the functional groups of DTPA, can be observed in the FT-IR spectrum of Al-DTPA, although there is an obvious red shift for these peaks. The presence of a broad FT-IR peak between 500 and 1000 cm^{-1} for Al-DTPA was ascribed to the formation of Al-O bonds in Al-DTPA (Figure S3).[59] The TGA curve under air shows that the amount of Al_2O_3 residues in total material at 800 °C is about 11.9 wt%, indicating a molar ratio of Al to DTPA of approximately 1:1 (Figure S4). These results sufficiently testified that the Al-DTPA should be formed by the direct coordination of DTPA and Al^{3+} in the molar ration of 1:1. The microfiber morphology of Al-DTPA may be resulted from the self-assembling of Al-DTPA with linear molecular structure through vander Waals interactions.[60]

3.2 Nitrogen-doped carbon microfibers

It is generally desirable but difficult to simultaneously modulate microstructures and morphologies of carbon materials toward the targeted functional properties and application, particularly for Nanoporous NCFs. Fortunately, Al-DTPA microfibers produced by a simple and scalable method can be used as cost-effective precursors (Figure 1) to obtain nitrogen-doped carbon microfibers. When being subjected to thermal treatment in nitrogen atmosphere above 750 °C, Al-DTPA microfibers are transformed to aluminium hydroxides or oxides-embedded carbon microfibers (Figure S5 A).

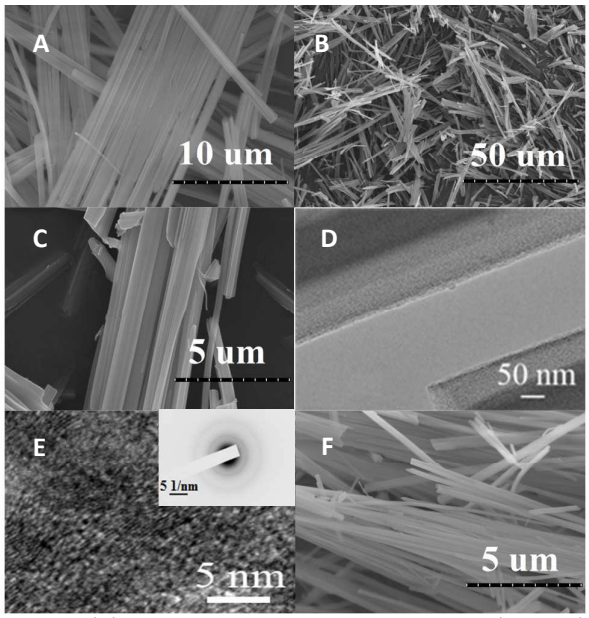

Figure 3 (A) SEM images for Al-DTPA microfibers; (B and C) SEM images of NCF-900; (D and E) TEM images of NCF-900. Inset is the corresponding selected area electron diffraction pattern of NCF-900; (F) SEM images for γ-Al_2O_3 obtained by heating Al-DTPA at 800 °C in air

These aluminium hydroxides or oxides served as the supports or hard-templates of carbon materials in the carbonization of Al-DTPA. It could avoid the excessive sinter and the agglomeration of carbon during the high-temperature carbonization of Al-DTPA. After leaching the aluminium hydroxide or oxides, NCFs with high surface area can be obtained at a scale of over 10 g (Figure 1 and S5 B). The TGA analysis for the NCF-900 indicates that almost no residues are observed after heating it at over 650 °C in air and that Al is completely removed in the prepared NCF-900. (Figure S6).

The microfiber morphology of Al-DTPA was still perfectly maintained in carbon materials after undergoing the calcination and acid-leaching (Figure 3B-E). The typical NCFs obtained at 900 °C have the diameters of ~500 nm and lengths of about 50-70 μm (Figure 3 B-D and S7). The XRD patterns for NCFs obtained above 750°C (Figure 1 b-c) displayed two obvious diffraction peaks at 2 θ values of 25 and 43 °, corresponding to (002) and (100) planes of graphitic carbons. The selected area electron diffraction patterns (SAED) of NCF-900 also reveal relatively clear diffraction-rings, indicating the formation of the graphitic carbon in the carbon frameworks. Some graphitization regions can be directly observed in the high-resolution TEM image of NCF-900 (Figure 3 E). However, the clearer graphite edges are difficult to be observed, owing to incomplete graphitization. A slight increasing in the graphitization-degree of carbon microfibers with increasing heat-treatment temperature can be observed in the XRD and SAED patterns (Figure2 and 3 E inset and Figure S8).

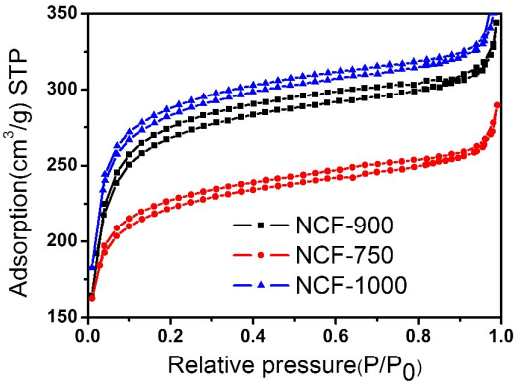

Figure 4 N_2-adsorption isotherm curves for nitrogen-doped carbon microfibers obtained at different temperatures

Table 1 Textual data of NCFs obtained at 750, 900 and 1000°C

Samples	S_{BET} (cm^2/g)	S_{meso} (cm^3/g)	S_{micro} (cm^3/g)	V_{total} (cm^3/g)	$V_{Micro}{}^T$ (cm^3/g)
750	604	84	520	0.39	0.28
900	933	108	825	0.58	0.43
1000	1072	67	1005	0.65	0.55

The nanoporous properties for the prepared NCFs at different temperatures can be directly observed in TEM images. Considerable interconnected pores are homogeneously distributed in the whole microfibers (Figure 3 D). The nitrogen-adsorption analysis (Figure 4) further confirms the nanoporous properties of NCF-900, with a broad hysteresis loop from 0.1 to 1.0 P/P_0 in the isothermal curves. The pore size distribution curves calculated from the adsorption branch of the isotherm curves using BJH method clearly showed the mesopores with detectable sizes of about 2-30 nm (Figure S9). These mesopores should be the cavities, left from the leaching of the particles of aluminium hydroxide or oxides. These mesopores can facilitate the transportation of O_2 and electrolyte solution during the ORR. Moreover, the micropores centred at 0.37 nm were found in these NCFs and generated from the carbonization of DTPA. These micropores can effectively adsorb O_2 molecules in the ORR catalysed by the carbon microfibers. The total BET surface area for NCF-750, -900, and -1000 are 604, 933 and 1072 $m^2 g^{-1}$, respectively (Table 1). This unique thermal conversion of Al-DTPA successfully prepared the NCFs with uniform fibre morphology, nanoporous structure, and appropriate degree of graphitization.

Actually, Al-DTPA microfibers can be also used as the precursors of γ-Al_2O_3 microfibers. After heat-treatment of Al-DTPA in air at 800 °C, the γ-Al_2O_3 with the well-defined microfiber morphology was observed in SEM images (Figure 3F) and further confirmed by XRD patterns (JSPDF 00-4557, Figure 2e). There is an obvious shrink in the diameter (~350 nm) and length (~60 μm), in contrast to those of Al-DTPA microfibers (Figure 3A). A low porosity of the γ-Al_2O_3 is observed by TEM, probably owing to the sintering in air at high temperature. It has smaller BET surface area (50 $m^2 g^{-1}$) and pore size distribution in the range of 2- 15 nm (Figure S10).

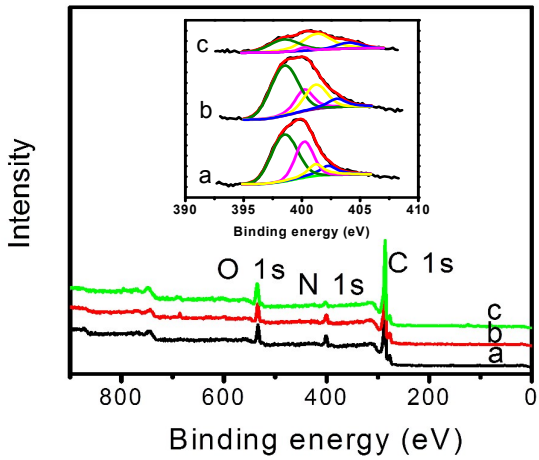

Figure 5 The XPS survey spectra and the deconvoluted N 1s XPS spectra (Inset) for NCF-750 (a), NCF-900 (b) and NCF-1000 (c)

Due to abundant nitrogen species in Al-DTPA precursors, nitrogen atoms with high content have been successfully doped into the resultant NCFs. The nitrogen contents in the surface of NCF-750, NCF-900, and NCF-1000 determined by XPS decreases with the increasing temperatures of heat treatment, in agreement with the results determined by elemental analysis (Figure 5 and Table S1). It is well known that nitrogen type in the carbon matrix is very influential on ORR activity of the nitrogen-doped carbon electrocatalysts. The N

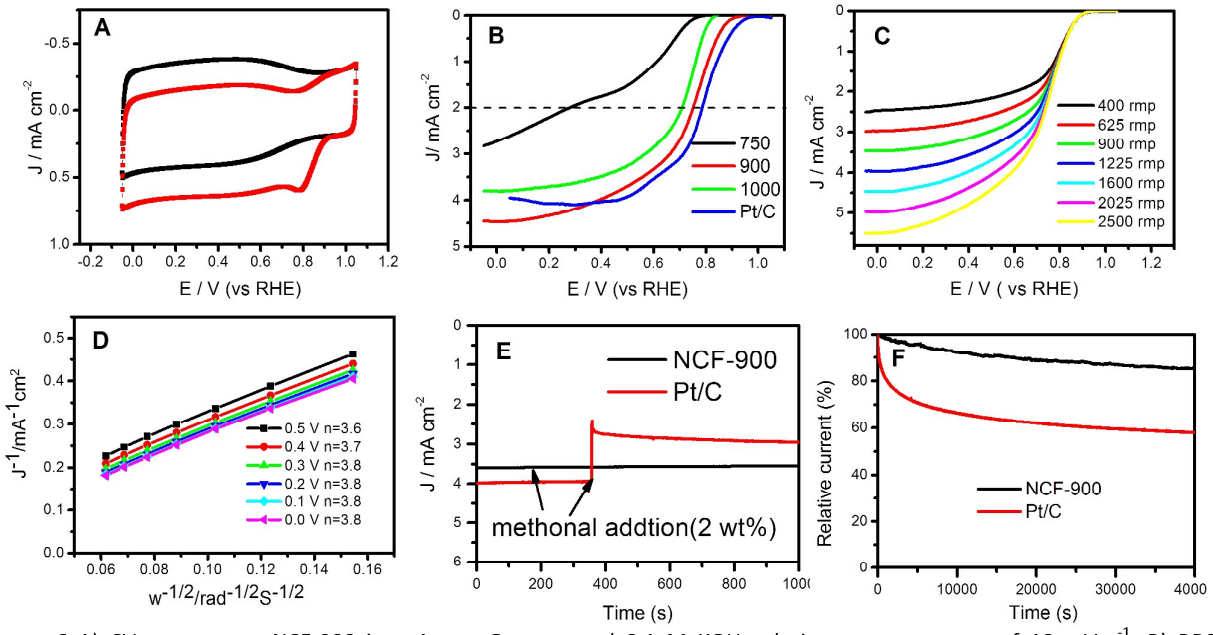

Figure 6 A) CVs on porous NCF-900 in a Ar- or O_2-saturated 0.1 M KOH solution at a scan rate of 10 mV s^{-1}; B) RDE voltammograms recorded on porous NCFs obtained at different temperatures and Pt/C (10 wt%) in 0.1 M O_2-saturated KOH solution; C) RDE voltammograms recorded on porous NCF-900 at different rotate speeds from 400 to 2500 rpm; D) K-L plots of J^{-1} versus ω^{-1} on porous NCF-900 at different potentials; E) current-time (i-t) plots for NCF-900 and Pt/C at 0.55 V in the presence of methanol; F) current-time (i-t) plots for NCFs-900 and Pt/C at 0.55 V in O_2-saturated KOH solution.

peaks at 398.3, 400.3, 401.2, and 403.6eV in the deconvoluted N1s XPS spectra are known to originate from pyridinic (at 398.3 eV), pyrrolic (at 400.3 eV), graphitic (at 401.2 eV) and oxidized type of (at 403.6 eV) nitrogen atoms, respectively (Figure 5 inset) The pyridinic- and graphitic-like nitrogen atoms [61], which are believed to be the main active sites for ORR, are dominant nitrogen types in NCF-900 (Table S1). The SEM EDS-mapping of NCF-900 intuitively illustrate well distribution of nitrogen ingredient in the whole microfibers (Figure S11). These results show that abundant pyridinic- and graphitic-like nitrogen atoms have been embedded in the graphitic matrixes of NCFs.

3.3 Oxygen electroreduction over NCFs

The characteristics of NCFs including high surface area, nanoporous structure, appropriate degree of graphitization, and plentiful nitrogen-doped carbon sites may enable NCFs to serve as efficient ORR electrocatalysts. Their electrocatalytic activities for ORR have been investigated in the Ar or O_2-saturated 0.1 M KOH solution in a conventional three-electrode system by CV and RDE voltammograms. In a Ar-saturated 0.1 M KOH solution, featureless voltammetric curves appear for NCFs, while prominent cathodic ORR peaks at about 0.8 V are observed in 0.1 M KOH electrolyte solution saturated with O_2, illustrating their effective ORR activity in alkaline medium (Figure 6 A). The NCFs prepared at different temperatures show the different ORR activity, in terms of their onset ORR potentials and half-wave potentials (Figure 6 B). Among them, the prepared NCF-900 displayed the most catalytic activity and possessed the half-wave potential of 0.75 V, very close to that over Pt/C (0.79 V). These facts testify that NCF-900 have a high catalytic activity for ORR in alkaline medium, comparable to the previously reported metal-free nitrogen-doped carbon materials.[39, 62] It may contribute to a combination of advantageous nitrogen content and type, high surface area, appropriate degree of graphitization for NCF-900. The ORR kinetic process on NCF-900 has been investigated by the RDE techniques. The corresponding K-L plots from the RDE curves (Figure 6 C and D) between 0.5 and 0.0 V exhibited good parallel straight lines, suggesting a reaction order of one with respect to oxygen in this potential range. According to the slope of the plots on the basis of the K-L equations, the number of electrons transferred is calculated to be 3.7 at 0.4 V (C_0=1.2×10^{-3}mol L^{-1}, D_0=1.9×10^{-5} cm s^{-1}, v= 0.01 cm^2 s^{-1}) meaning that NCF-900 can nearly catalyse a 4-electron oxygen reduction reaction in 0.1 M KOH.[63]

The NCF-900 was demonstrated to have better methanol-tolerant property than Pt/C materials. The significant impact of methanol on ORR current density over Pt/C cathode was observed in the corresponding (I-T) curve after methanol were added (Figure 6 E). No noticeable changes were found in the ORR current over NCF-900 in the presence of methanol (3 wt%). Moreover, the durability of NCF-900 during ORR is superior to Pt/C materials, and the corresponding I-T plots for NCF-900 exhibited a relative slow attenuation (Figure 6 F). A high relative current of about 85 % in 0.1 M KOH solution still persisted after 40,000s. However, Pt/C electrodes showed a current density decrease (to approximately 58 %) in 0.1 M KOH solution after 40,000 s.

Table 2 Acid amount of SO_3H/NCF prepared at different carbonization temperatures

calcination temperature（°C）	acid amount（mmol/g）	SO_3H-（mmol/g）	COOH-（mmol/g）	OH-（mmol/g）
300	1.2	0.8	0.2	0.2
400	1.1	0.9	0.1	0.1
500	1.4	1.2	0.1	0.1
600	2.0	1.6	0.2	0.2
700	1.8	1.5	0.1	0.2
800	1.4	1.2	0.1	0.1
900	1.0	0.8	0.1	0.1

3.4 Sulfonated carbon microfiber as solid acids

As a green and easily recycled acid catalyst, sulfonated carbon has received much attention in various acid-catalysed reaction systems.[64] Sulfonated carbon microfibers with highly porous structures are not only favourable for reactant accessibility to active sites, but also particularly easily separated from solution by filtration. However, sulfonated carbon acids with nanoporous structure, microfiber morphology, and higher acid density are very rarely reported. In our synthesis, Al-DTPA microfibers were carbonized at the chosen temperatures in order to provide a hydrophilic, active but stiff surface for the covalently grafting of SO_3H groups. Al-DTPA-derived microfibers may result in unstable surface structure when carbonized at lower temperature. However, after undergoing heat-treatment at higher temperature, the increased cross-linking polycyclic aromatic carbon structures would prevent incorporation of H_2SO_4 into the NCF surface. The most

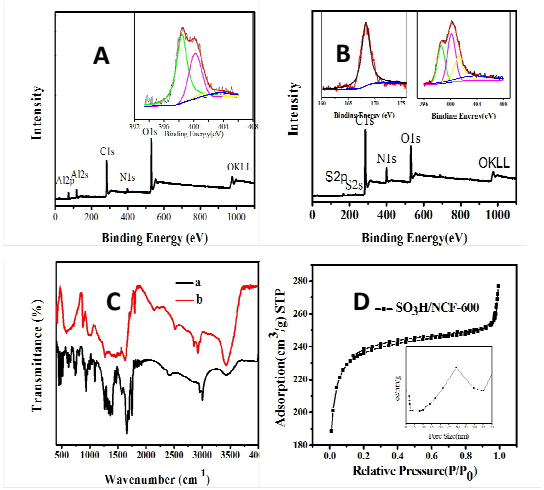

Figure 7 (A) XPS survey spectra and the deconvoluted N 1s XPS spectra(Inset), for NCF-600; (B) XPS survey spectra and the deconvoluted N 1s XPS spectrum(Inset on the right), S 2p XPS spectrum (Inset on the left) for SO_3H/NCF-600; (C) FT-IR spectra for SO_3H/NCF-600 a and NCF-600 b; (D)N_2-adsorpotion-desorpotion isotherms of SO_3H/NCF-600 and the BJH pore size distribution curves(Inset).

optimized carbonization temperature for the preparation of Al-DTPA-derived carbon-based acid is 600 °C, which is determined to contain -SO_3H (1.6mmol g^{-1}), -OH (0.2 mmol g^{-1}), and -COOH (0.2 mmol g^{-1}) group on the carbon surface. The -SO_3H acid density of SO_3H/NCF-600 is higher than sulfonated graphene and carbon nanotubes prepared by the similar method.[65-66] High acid density is possibly related to the nitrogen-doped carbon surface, because doping nitrogen atoms in the carbon surface may easily serve as the alkalinity sites or chemically active defects for the grafting of -SO_3H groups and thus enhance the acid density.

The successful grafting of SO_3H groups on the NCFs was demonstrated by FT-IR, XPS, SEM, EDS, and element analysis (Figure 7). IR absorption bands at about 1008, 1030 and 1120 cm^{-1} could be observed in the FT-IR spectrum (Figure 7 C) of the sulfonated carbons, assigning to the symmetric stretching vibrations of S=O (or S-OH) .[63-65] There is another additional absorption band at 520 cm^{-1} due to the stretching vibration of C-S. [64] The XPS and SEM-EDS measurements indicated that C, N, O and S elements are the main ingredients of surfonated NCFs. (Figure 7A and S12). Aluminium oxide or hydroxide embedded in nitrogen-doped carbon microfibers were successfully leached by H_2SO_4 in the sulfonation (Figure 7A and B). The symmetrical peak at 168.8 eV ascribing to sulfur were observed in the XPS spectrum of SO_3H/NCF-600 (Figure 7 B), suggesting the successful grafting of SO_3H groups on the surface of NCFs. [62-65] After undergoing the sulfonation, nitrogen species on the surface of NCFs have changed, and quaternary ammonium-type nitrogen atoms remarkably increased (Figure 7 A and B. N1s spectra; Table S1 and S2). This phenomenon might be related to the surface sulfonation of NCFs, in agreement with the enhanced acid density. It implies that SO_3H functional groups may be grafted on the N atoms of NCFs or these N atoms were protonized in sulfonation. Moreover, a microfiber morphology of the sulfonated samples is still maintained and the sulfonation seems to not destroy the microfiber morphology of carbon (Figure S12).

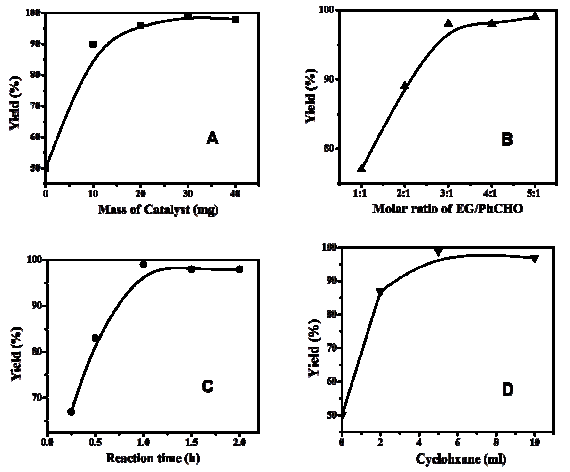

Figure 8 (A) The effect of catalyst amount on the yield of acetal (reactant: EG, 2.79 g; PhCHO, 1.59 g; solvent:cyclohexane, 5.0 g; and reaction time, 1 h); (B) The effect of molar ratio of EG/PhCHO on the yield (solvent: cyclohexane, 5.0 g; catalyst: SO_3H/NCF-600, 30 mg; and reaction time, 1h); (C) The effect of reaction time on the yield of acetal (solvent: cyclohexane, 5.0 g; reactant: EG, 2.79 g; PhCHO, 1.59 g; and catalyst: SO_3H/NCF-600,30 mg S); (D) The effect of cyclohexane amount on the yield of acetal (reactant: EG, 2.79 g; PhCHO, 1.59 g; catalyst: SO_3H/NCF-600, 30 mg; and reaction time, 1 h)

It is well-known that abundant porosity is extremely beneficial for the enhancement of acid amount and catalytic performance. However, the reported carbon-based solid acids often have a lower surface area and absent larger-pore (>2 nm) property. The prepared sulfonated SO_3H/NCF-600 by us has a BET surface area of 921 m^2 g^{-1}, higher than sulfonated graphene solid acids. [65-67] The pore size-distribution curves of SO_3H/NCF-600 revealed a mesopore size distribution in the range of about 10-40 nm. The large-pore porosity of SO_3H/NCF-600 may be attributed to the removal of Al_2O_3 or aluminium hydroxide nanoparticles carved in the NCFs. In the H_2SO_4-solvothermal treatment process, these nanoparticles may leave numerous cavities and facilitate the formation of highly nanoporous structures. These results indicated that the -SO_3H acid functional groups should be incorporated into the accessible pores of NCFs, contributing to the enhancing of protonic acid density.

The synthesized SO_3H/NCF-600 was used to catalyse the typical acetalization reaction of EG and PhCHO, giving acetal as the final products (Figure 8). In the acetalization of EG with PhCHO, water as the only byproduct was produced. Cyclohexane was used as an agent entraining water to improve the yield of acetal by removing water produced from reaction system at the refluxing temperature (about 90 °C). From the results in Figure 8, it can be found that the amount of catalyst and cyclohexane, EG to PhCHO molar ratio, and reaction time can significantly change the yield of acetal. The highest yield (99 at%) was obtained at the following reaction conditions: 30 mg SO_3H/NCF-600, EG/PhCHO molar ratio of 5:1, and the reaction time of 1h. The catalytic efficiency of SO_3H/NCF-600 based on the same catalyst amount is higher than starch-derived carbon-based strong acids.[68] Moreover, this SO_3H/NCF-600 catalyst could be very easily separated from the reaction mixtures by filtration. After washing with ethanol and water, this solid acid can be reused as catalysts for next run. It was found that the catalytic efficiency of this carbon solid acid is almost not changed (Figure S13). After the SO_3H/NCF-600 catalysts were recycled 5 times, the yield of the acetal was not yet decreased at the same reaction condition. These results indicated that SO_3H/NCF-600 are high-efficiency and easily recycled acid catalyst for the acetalization reaction of EG and PhCHO.

4 Conclusions

In summary, this research work presented a facile synthesis pathway to prepare nanoporous nitrogen-doped carbon

microfibers. A simple homogeneous precipitation reaction of DTPA and Al salts produced Al-DTPA coordination polymer microfibers at a synthesis scale of 0.25 kilograms in laboratory. The subsequent carbonization at different temperatures resulted into the formation of NCFs with a scale of over 10 g. The NCFs obtained at 900 °C show a high catalytic activity for ORR, comparable to the reported metal-free carbon electrocatalysts in alkaline medium. Moreover, the sulfonation of NCFs can successfully graft -SO_3H sulfonic groups on the surface of NCFs, which was a high-efficiency and recycled nanoporous solid acids in acetalization reaction of benzaldehyde with ethylene glycol. This simple and scalable synthesis method offered a new and industrially available route to obtain nanoporous nitrogen-doped carbon microfibers, which can be developed as efficient metal-free ORR electrocatalyst and solid acids.

Acknowledgements

The authors are grateful for financial support from the National Natural Science Foundation (No.21303058), the Shanghai Municipal Natural Science Foundation (No. 13ZR1412400) and the key project of Shanghai Science and Technology Committee (No. 11JC1403400;14231200300).

Notes and references

1 Y. Yan, J. Miao and Z. Yang, Chem. Soc. Rev., 2015, 44, 3295 -3346.
2 X. Xu, H. Li and Q. Zhang, ACS nano, 2015, 9, 3969-3977.
3 J. Tang, R. R. Salunkhe and J. Liu, J. Am. Chem. Soc., 2015, 137, 1572-1580.
4 L. K. Shrestha, R. G. Shrestha and Y. Yamauchi, Angew. Chem., 2015, 127, 965-969.
5 L. Wang, X. Feng and L. Ren, J. Am. Chem. Soc., 2015, 137, 4920-4923.
6 A. Kaushik, R. Kumar and S. K. Arya, Chem. Rev., 2015, 115, 4571 -4606.
7 J. Hou, C. Cao and F. Idrees, ACS Nano, 2015, 9, 2556-2564.
8 S. Gao, H. Liu and K. Geng, Nano Energy, 2015, 12, 785-793.
9 K. Sakaushi, T. P. Fellinger and M. Antonietti, ChemSusChem, 2015, 8, 1156-1160.
10 J. Zhang, Z. Zhao and Z. Xia, Nature Nanotech. 2015, 10, 444-452.
11 Z. Ma, S. Dou and A. Shen, Angew. Chem., 2015, 127, 1908-1912.
12 L. Hao, S. Zhang and R. Liu, Adv. Mater., 2015, 27, 3190-3195.
13 E. F. Holby and C. D. Taylor, Sci. Rep., 2015, 5, 9286.
14 W. Yuan, J. Li and A. Xie, Electrochim. Acta, 2015, 165, 29-35.
15 J. Shui, M. Wang and F. Du, Sci. Adv., 2015, 1, e1400129.
16 H. Watanabe, S. Asano and S. Fujita, ACS. Cata., 2015, 5, 2886 -2894.
17 H. W. Liang, Z. Y. Wu and L. F. Chen, Nano Energy, 2015, 11, 366-376.
18 Y. Gong, H. Fei and X. Zou, Chem. Mater., 2015, 27, 1181-1186.
19 Y. Nie, L. Li and Z .Wei, Chem.Soc. Rev., 2015, 44, 2168-2201.
20 X. Liu, Y. Zhou and W. Zhou, Nanoscale, 2015, 7, 6136-6142.
21 H .Watanabe, S. Asano and S. Fujita, ACS. Cata., 2015, 5, 2886 -2894.
22 Y. A. Zehtab, K. Chizari and A. Jalilov. ACS. Nano., 2015, 9, 5833 -5845.
23 E. Haque, M. M. Islam and E. Pourazadi, RSC. Adv. 2015, 5, 30679-30686.
24 Y. Chen, R. Ma and Z .Zhou, Adv. Mate. Inter., 2015, 9, 5833-5845.
25 G. A. Ferrero, M. Sevilla and A. B. Fuertes, Carbon, 2015, 88, 239-251.
26 C .Wang, Y .Li and X. He, Nanoscale, 2015, 7, 7550-7558.
27 J. Hou, C .Cao and F. Idrees, ACS. Nano, 2015, 9, 2556-2564.
28 A. L. Wang, X. J. He and X. F. Lu, Angew. Chem. Int. Ed., 2015, 54, 3669-3673.
29 X. Gu, C. Lai and F. Liu, J. Mater. Chem. A., 2015, 3, 9502-9509.
30 C. Wang, H. Wang and C. Zhai, J. Mate. Chem. A, 2015, 3, 4389 -4398.
31 A. Olejniczak, M. Leżańska, A. Pacuła, Carbon, 2015, 91, 200-214.
32 Y. Sun, R. B. Sills and X. Hu, Nano. Lett., 2015, 15, 3899-3906.
33 J. Huang, J. Wang and C. Wang, Chem. Mater., 2015, 27, 2107-2113.
34 G. Sun, X. Zhang, R. Lin, Angew. Chem., 2015, 127, 4734-4739.
35 T. Y. Ma, J. Ran and S. Dai, Angew. Chem., 2015, 54, 4646-4650.
36 Z. Zhang, F. Xiao and S. Wang, J. Mater. Chem. A, 2015, 3, 11139-11670.
37 J. Yin, Y. Qiu, J. Yu, Chem. Lett., 2013, 42, 413-415.
38 J. Yin, Y. J. Qiu and J. Yu, Rsc. Adv., 2013, 3, 15655-15663.
39 Y. Qiu, J. Yu and T. Shi, J. Power Sources, 2011, 196, 9862-9867.
40 J. Yuan, A. G. Marquez and J. Reinacher, Poly. Chem., 2011, 2, 1654-1657.
41 Y. R. Fan, Z. B. Zhao and Q. Zhou, Carbon, 2013, 58, 128-133.
42 S. Lim, S. H. Yoon and I. Mochida, Langmuir, 2009, 25, 8268-8273.
43 T. M. Minea, S. Point and A. Granier, Appl. Phys. Lett., 2004, 85, 1244-1246.
44 D. S. Yang, S. Chaudhari and K. P. Rajesh, ChemCatChem, 2014, 6, 1236-1244.
45 G. S. Park, J. S. Lee and S. T. Kim, J. Power Sources, 2013, 243, 267-273.
46 J. Wei, Y. Liang and X. Zhang, Nanoscale, 2015, 7, 6247-6254.
47 Q. Shi, R. Zhang and Y. Lv, Carbon, 2015, 84, 335-346.
48 S. Zhang, A. Ikoma and K. Ueno, ChemSusChem, 2015, 8, 1608-1617.
49 M. M. Titirici, R. J. White and N. Brun, Chem. Soc. Rev., 2015, 44, 250-290.
50 Q. Tian, Z. Zhang and L. Yang, Carbon, 2015, 93, 887-895.
51 A. Béziau, S. A. Baudron and G. Rogez, Inorg. Chem., 2015, 54, 2032-2039.
52 C. P. Li, J. Chen and C. S. Liu, Chem. Commun., 2015, 51, 2768 -2781.
53 R. Matsuoka, R. Toyoda and R. Sakamoto, Chem. Sci., 2015, 6, 2853-2858.
54 Y. Ye, L. Zhang and Peng Q, J. Am. Chem. Soc., 2015, 137, 913 -918.
55 C. R. Murdock and D. M. Jenkins, J. Am. Chem. Soc., 2014, 136, 10983-10988.
56 W. Xia, A. Mahmood and R. Zou, Energy Environ. Sci., 2015, 8, 1837-1866.
57 S. Suganuma, K. Nakajima and M. Kitano, J. Am. Chem. Soc., 2008, 130, 12787-12793.
58 A. Kong, X. Zhu and Z. Han, ACS. Catal., 2014, 4 , 1793-1800.
59 S. Lukić, I. Stijepović and S. Ognjanović, Ceram. Int. 2015, 41, 3653-3658.
60 W. Li, F. Zhang and Y. Dou, Adv. Energ. Mater. 2011, 1, 382-386.

61 L. Qu, Y. Liu and J. B. Baek, ACS. Nano, 2010, 4, 1321-1326.
62 D. S. Yang, S. Chaudhari and K. P. Rajesh, Chem. Cat. Chem., 2014, 6, 1236-1244.
63 A. Kong, X. Zhu and, Z. Han, ACS. Catal., 2014, 4 , 1793-1800.
64 P. Gupta and S. Paul, Catal. Today, 2014, 236, 153-170.
65 F. Liu, J. Sun and L. Zhu, J. Mater. Chem., 2012, 22, 5495-5502.
66 H. Yu, Y. Jin and Z. Li, J. Solid. State. Chem., 2008, 181, 432-438.
67 Z. Wei, Y. Yang and Y. Hou, Chem. Cat. Chem., 2014, 6, 2354-2363.
68 X. Liang, C. Li and C. Qi, J. Mater. Sci., 2011, 46, 5345-5349.

Al-coordination polymers-derived nanoporous nitrogen-doped carbon microfibers as metal-free catalysts for oxygen electroreduction and acetalization reaction

Zhen Han[a,b],Youyi Yu[a],Yongbo Zhang[a], Bing Dong[a], Aiguo Kong*[a]and Yongkui Shan*[a]

a, School of Chemistry and Molecular Engineering, East China Normal University, 500 Dongchuan Road, Shanghai 200241, P.R. China.

b, Shanghai Key Laboratory of Molecular Catalysts and Innovative Materials, Fudan University, Shanghai 200433, P.R. China.

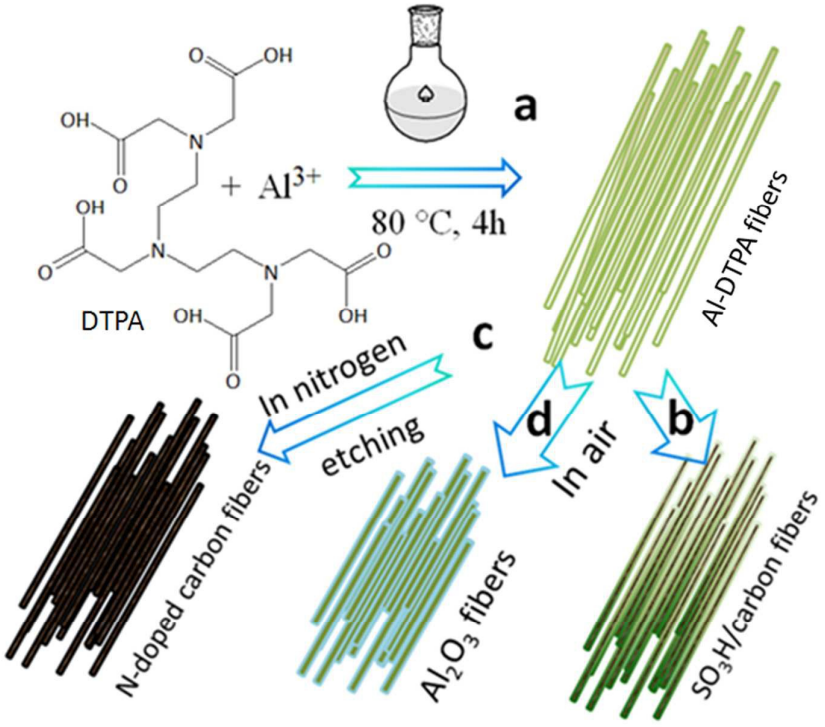

Nanoporous nitrogen-doped carbon microfibers were prepared by thermal conversion of aluminium-diethylenetriamine pentaacetatic acid coordination polymers on a large scale, which could be used as efficient oxygen electroreduction catalysts and to prepare porous solid acid catalysts for the acetalization reaction.